https://doi.org/10.20965/jdr.2019.p0315

Survey Report:

Development of a Real-Time Damage Estimation System

Hiroyuki Fujiwara[*1,†], **Hiromitsu Nakamura**[*1], **Shigeki Senna**[*1], **Hideyuki Otani**[*2], **Naoya Tomii**[*3], **Kiyonori Ohtake**[*4], **Toshiya Mori**[*5], **and Shojiro Kataoka**[*6]

[*1]Research Center for Reinforcement of Resilient Function, National Research Institute for Earth Science and Disaster Resilience
3-1 Tennodai, Tsukuba-shi, Ibaraki 305-0006, Japan
[†]Corresponding author, E-mail: fujiwara@bosai.go.jp
[*2]Computational Disaster Mitigation and Reduction Research Team, RIKEN Center for Computational Science, Hyogo, Japan
[*3]Satellite Appications and Operations Center, Space Technology Directorate I, Japan Aerospace Exploration Agency (JAXA), Ibaraki, Japan
[*4]Applications Laboratory, Resilient ICT Research Center, National Institute of Information and Communications Technology, Kyoto, Japan
[*5]Geochemical Research Center, Graduate School of Science, The University of Tokyo, Tokyo, Japan
[*6]Earthquake Disaster Management Division, Road Structures Department,
National Institute for Land and Infrastructure Management, Ministry of Land, Infrastructure, Transport and Tourism, Ibaraki, Japan
[Received August 20, 2018; accepted January 31, 2019]

Assessing the extent of damage quickly following a major natural disaster is crucial to ensuring that effective decisions are made to establish an appropriate first response system and implement response measures. Therefore, a real-time earthquake damage estimation system was developed. Among other things, the system estimates the distribution of seismic ground motion, structural damage, and casualties based on observation records obtained immediately after a major earthquake. In addition, the system is equipped with a function for assessing actual damage using a variety of sources and techniques. Damage estimates generated by the system were used for emergency response during actual disasters, including the 2016 Kumamoto Earthquakes, and the system's effectiveness has been confirmed. This study evaluates the functions and performance of the system, examines its potential applications, and discusses future innovations and challenges.

Keywords: natural disaster, disaster response, damage estimation, damage assessment

1. Introduction

Japan has been hit by a series of large-scale earthquake disasters in recent years, including the 1995 Hanshin-Awaji Earthquake and the 2011 Great East Japan Earthquake. In addition to earthquakes, many other natural disasters have also struck the nation, including the 2014 Hiroshima landslides, eruption of Mt. Ontake, 2015 heavy rainfalls in the Kanto and Tohoku regions, and 2018 torrential rain and landslides in western Japan.

As a country susceptible to natural disasters, we face an urgent need to apply the lessons we learned from past disasters to prepare ourselves for potential large-scale disasters and to build a resilient society capable of ensuring the safety and security of citizens. The basic principle of disaster management is to develop countermeasures by anticipating potential hazards in advance. It is crucial, therefore, that damage be quickly assessed when a disaster strikes so that the information can be used to establish a first response system and take disaster response measures.

In this study, we conducted research and development on a real-time damage estimation system capable of providing an overview of damage by estimating and assessing damage on a real-time basis, even in the event of a disaster affecting extensive areas, such as a major earthquake, while providing detailed damage estimation applicable to individual towns and buildings. In addition, we engaged in research and development with the aim of not only estimating damage but also gathering and analyzing disaster information through various means.

Specifically, we worked on the following research and development themes (see **Fig. 1**).

1. Development of a real-time damage estimation and data application system
2. Development of high-resolution damage estimation technology using structural analysis
3. Research and development related to disaster information extraction using earth observation satellites
4. Development of the Disaster Information Summarization System using social media
5. Development of a real-time monitoring technology for volcanic gases and ash

Results will be described below.

2. Development of a Real-Time Damage Estimation System

2.1. System Overview

An overview of the system is shown in **Fig. 2**. The seismic motion inputs required for estimating damage are

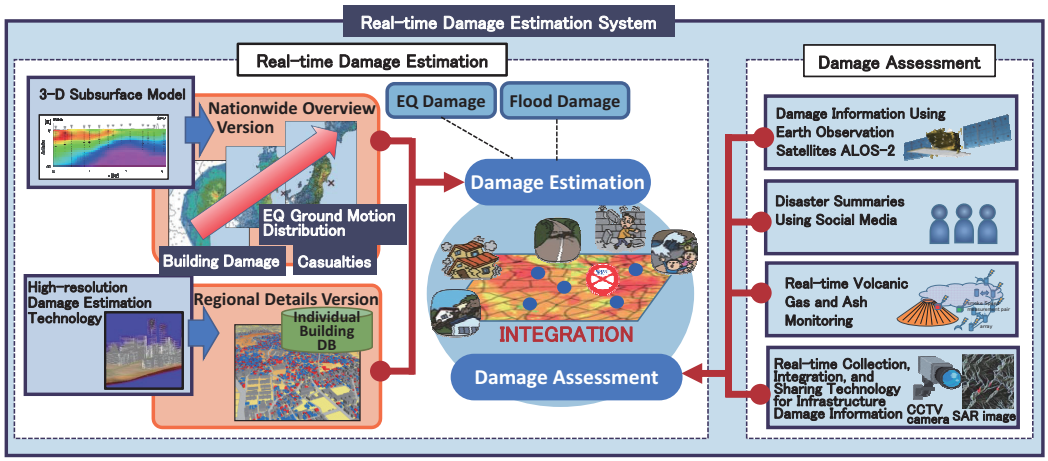

Fig. 1. Outline of research and development.

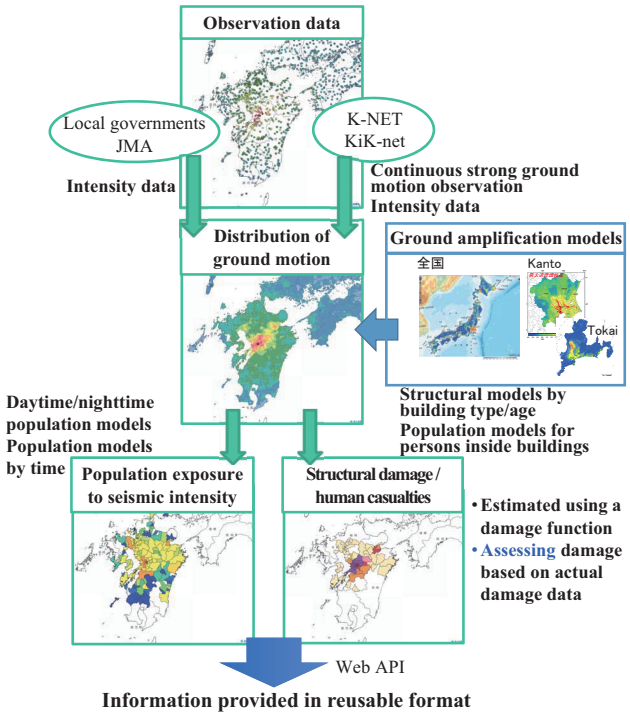

Fig. 2. A schematic of the real-time damage estimation system.

obtained as follows. We receive a wide range of ground motion data from a total of approximately 5,300 observation points, including data recorded by K-NET and KiK-net, the nationwide strong-motion seismograph networks operated by the National Research Institute for Earth Science and Disaster (NIED), and seismic intensity measurements recorded by local government organizations and the Japan Meteorological Agency (JMA). Then using the site amplification factors provided by the Japan Seismic Hazard Information Station (J-SHIS), as well as those obtained from wide-area subsurface models covering the Kanto and Tokai areas described in the next section, the distribution of ground motion is estimated for each of the 250-m grid cells (totaling approximately 6 million grid cells nationwide) in terms of seismic intensity, peak ground acceleration (PGA), peak ground velocity (PGV), SI value, and velocity response spectrum, among others.

On the basis of the estimated ground motion distribution, population exposure to seismic intensity is derived using the number of persons who are inside buildings during daytime, nighttime, and specific time windows. In addition, structural damage – including numbers of completely and partially destroyed buildings – will be estimated by using the estimated ground motion distribution and nationwide structural models with attributes necessary for estimating damage and by applying damage functions.

Further, casualties will be estimated on the basis of structural damage. Population models for persons who are inside buildings will be constructed for each time window by taking into account statistical data on the number of persons in transit. Multiple structural damage functions and human casualty functions will be applied to estimate the numbers of persons killed, severely injured, and moderately injured.

As a rule, these damage estimation processes are performed when a seismic intensity of approximately 3 or more is detected. Then, data are dispatched roughly 10 minutes after an earthquake and are detected in such formats that can be put to secondary use via Web Application Programming Interface (API).

Further, the system is equipped with a damage estimation function to improve estimation accuracy. A model is constructed for errors in damage function parameters using probability variables. Then, the Bayesian update is performed on the parameters of the probability distribution using the actual number of damaged buildings obtained following the disaster from some parts of the estimated area.

While it is difficult to make a general comparison between our system and disaster response systems adopted

by central and local governments, some of the most characteristic features of our system can be described as follows:

- The system is capable of gathering data recorded by the seismometers of the NIED's K-NET and KiK-net, the JMA, and local governments, and then estimating seismic ground motion, structural damage, and casualties nationwide in units of 250-m grid cells.
- Outputs from ground motion estimation include not only seismic intensity but also a broad range of data including peak ground velocity, peak ground acceleration, and spectral intensity.
- Estimated results are published on a website immediately after an earthquake, and data are generated in a reusable format to facilitate application across society.

2.2. Estimating Ground Motion

Ground motion data that serve as input for each evaluation point are needed to estimate earthquake damage. In many cases, however, there are no observation points located in close proximity to the evaluation point and on ground comparable to that of the evaluation point. For this reason, ground motion over a spatially extensive area must be estimated based solely on ground motion recorded at observation points.

In addition to intensity-related information (intensities at 10-second intervals, intensities at 1-minute intervals, real-time intensities), the system receives PGVs, PGAs, SI values, acceleration response spectra, and velocity response spectra as observation data from the K-NET and KiK-net observation points. The system also receives the JMA intensity measurement data recorded by local governments and the JMA. These observation data are not transmitted simultaneously after an earthquake, but is sent individually in any order from each observation point as the seismic motion spreads. Once the number of intensity measurements of 2.5 or above received from the K-NET and KiK-net observation sites exceeds a threshold within a prescribed time period, the system switches to estimation mode and begins estimating damage.

To estimate seismic intensities over extensive areas using spatial interpretation, an empirical equation is used to derive PGVs based on the seismic intensity data observed at ground surface level. Then, PGVs at engineering bedrock are estimated by accounting for the amplification factor at each observation site. We estimated the spatial distribution in each 250-m grid cell by interpolation using inverse distance weighting (IDW) and multiplying the result by the amplification factor again [1]. For nationwide estimates, the amplification factors published by J-SHIS were used [2], while the amplification factors referred to in Section 2.8 [3] were used to estimate damage in the Kanto and Tokai areas. Along with seismic intensities, the system also estimates PGVs, PGA, SI values, acceleration response spectra, and velocity response spectra.

2.3. Estimating Structural Damage

Building models were constructed on the basis of buildings across Japan to estimate damage. We used residential maps (Zenrin's Zmap-Town II) generated on the basis of on-site surveys covering nearly all areas of Japan. For each 250-m grid cell, we developed building models (for approximately 56 million buildings) equipped with attributes necessary to estimate damage, such as structural category and age. Using the technique established by Oi et al. [4] as reference, we enhanced the accuracy of damage estimation as described below.

Using the building type assigned to each building in the residential map data, the buildings are categorized as residential or commercial and assessed structurally (wood, steel, reinforced concrete). In this assessment, the structural categories used in real estate information (on approximately 1.7 million buildings) available in the private sector are sorted into wood, steel, reinforced concrete, and buildings (**Table 1**).

In addition, the number of buildings in each age group is estimated for each structural type using the 19 age categories found in the "Survey of Buildings Based on Table 38 Age Categories" in the Preliminary Survey of Real Properties in Japan (**Table 2**).

Fig. 3 shows the nationwide distribution of building categories estimated as described above.

Structural damage is estimated to be either "completely destroyed" or "partially destroyed" by inputting the estimated ground motion and applying damage functions to the building models described above. As shown in **Table 3**, several damage functions are applied to each of the structural categories. By developing eight patterns of combinations, the system is able to generate a broad range of damage estimates.

2.4. Estimating Casualties

We developed population models for the number of persons inside buildings, which are required to estimate casualties attributed to structural damage. We classified the population estimated to be inside each grid cell into persons at home, persons inside buildings other than their home, and persons in transit to establish population models for persons inside buildings during each time window. The number of persons at home and inside buildings other than their home was estimated for each 250-m grid cell from grid-based regional statistics from the 2010 National Census, grid-based regional statistics from the 2009 Basic Survey for Economic Census, the 2011 Basic Survey on Time Use and Leisure Activities, and the number of students by school type (kindergarten to graduate school) [13].

The number of persons in transit during each time window was calculated for each grid cell using the 2011 Basic Survey on Time Use and Leisure Activities, data on persons in transit derived from GPS location information using smartphone apps [14], and 2012 statistics on passengers boarding and alighting trains by station, while taking into account the distribution of rental buildings and

Table 1. Structural classification assessment table.

Attribute type		No. of stories		Building type	Structural category	Floor area per building	Structural category
No name		No. of stories	2 or less	(Target structure)		–	RC
				(Detached)		Less than 200 m^2	Wood
				–		200 m^2 or more	Steel

Attribute type		No. of stories		Floor area per building	Structural category
Name found	Target structure	No. of stories	2 or less	Less than 80 m^2	Wood
		No. of stories	1 or more	–	RC

Attribute type		No. of stories		Floor area per building	Structural category
Name found	Rental building	No. of stories	2 or less	Less than 150 m^2	Wood
		No. of stories		150 m^2 or more	Steel
		No. of stories	3, 4	Less than 50 m^2	Steel
		No. of stories		50 m^2 or more	RC
		No. of stories	5 or more	-	RC

Attribute type		No. of stories		Floor area per building	Structural category
Name found	Multi-family building	No. of stories	1	-	Wood
		No. of stories	2	Less than 200 m^2	Wood
				200 m^2 or more	Steel
		No. of stories	3	Less than 150 m^2	Steel
				150 m^2 or more	RC
		No. of stories	4 or more	-	RC

Attribute type		No. of stories		Floor area per building	Structural category
Name found	Residential home	No. of stories	2 or less	-	Wood
		No. of stories	3 or more	Less than 50 m^2	Wood
				50 m^2 or more	RC

Attribute type		No. of stories		Floor area per building	Structural category
Name found	Office	No. of stories	2 or less	Less than 50 m^2	Wood
				50 m^2 or more	Steel
		No. of stories	3	-	Steel
		No. of stories	4 or more	-	RC

Table 2. Age categories of building models.

Category	Age category in Preliminary Survey of Real Properties in Japan
Category 1	Proportion of buildings completed on January 1, 1963 or before
Category 2	Proportion of buildings completed between January 2, 1963 and January 1, 1972
Category 3	Proportion of buildings completed between January 2, 1972 and January 1, 1981
Category 4	Proportion of buildings completed between January 2, 1981 and January 1, 1990
Category 5	Proportion of buildings completed between January 2, 1990 and January 1, 2002
Category 6	Proportion of buildings completed between January 2, 2002 and January 1, 2011
Category 7	Proportion of buildings completed between January 2, 2011 and January 1, 2014

offices based on structural type obtained from residential map data.

Using the estimated number of persons at home and persons inside buildings other than their home as the number of persons inside buildings, and combining it with damage functions to be applied to estimate structural damage, we generated eight patterns of casualty estimates shown in **Table 4**. We also provided a broad range of estimation results as was done with the estimates for structural damage. It is important to note, however, that types of estimated casualties may vary depending on the casualty function used, as shown in **Table 5**.

2.5. Providing the Results of Damage Estimation

Results of estimated damage are visualized on a members-only website using WebGIS, allowing users to view data by superimposing it on a standard online mapping service. An example of the search results page is shown in **Fig. 4**. Users can do a search on damage estimates using keywords such as the location of the epicenter and information related to the hypocenter, along with time period, maximum seismic intensity recorded, and number of observation points. Search results are shown in a list and displayed as a 250-m grid diagram corresponding to the selected results (e.g., ground motion, population expo-

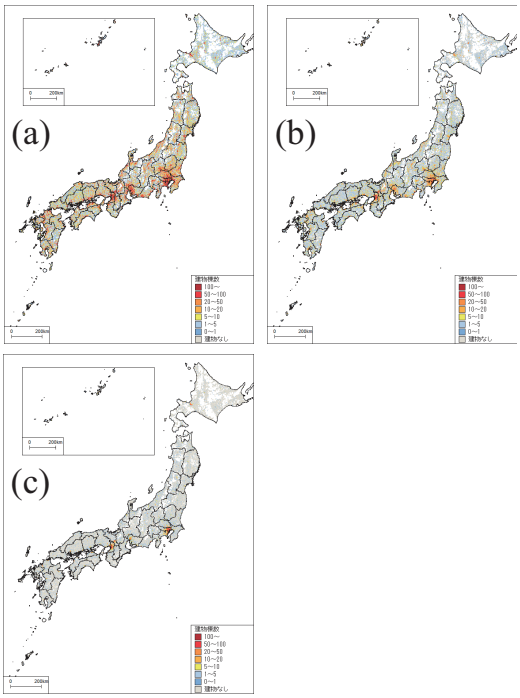

Fig. 3. Nationwide distribution of building categories ((a) Wood, (b) Steel, (c) RC).

Table 3. List of techniques for estimating structural damage.

Method	Structure	Reference
M1	Wooden	Central Disaster Management Council (2012) [5]
	Reinforced-Concrete	
	Steel	
M2	Wooden	Horie (2004) [6] D4,D2
	Reinforced-Concrete	Murao and Yamazaki (2002) [7]
	Steel	Murao and Yamazaki (2002) [7]
M3	Wooden	Horie (2004) [6] D3,D1
	Reinforced-Concrete	Murao and Yamazaki(2000) [8]
	Steel	Murao and Yamazaki(2000) [8]
M4	Wooden	Murao and Yamazaki (2002) [8]
	Reinforced-Concrete	
	Steel	
M5	Wooden	Central Disaster Management Council (2004) [9]
	Reinforced-Concrete	
	Steel	
M6	Wooden	Saeki et al. (2016) [10]
	Reinforced-Concrete	
	Steel	
M7	Wooden	Midorikawa et al. (2011) [11]
	Reinforced-Concrete	
	Steel	
M8	Wooden	Shimizu et al. (2016) [12]
	Reinforced-Concrete	
	Steel	

Table 4. List of techniques for estimating casualties.

Model	Reference	Method for building damage (**Table 3**)
P1	Central Disaster Management Council (2012) [5]	M1
P2	Central Disaster Management Council (2012) [5]	M6
P3	Saeki et al. (2001) [15]	M1
P4	Saeki et al. (2001) [15]	M6
P5	Okada and Nakashima (2015) [16]	Okada and Nakashima (2015) [16]
P6	Saeki et al. (2001) [15]	M4
P7	Central Disaster Management Council (2012) [5]	M8
P8	Saeki et al. (2001) [15]	M8

Table 5. List of types of casualties estimated.

Method	Casualty
P1, P2, P7	Deaths, severely injured, moderately injured, persons requiring assistance for evacuation, evacuees (impact of critical infrastructure is not taken into account)
P3, P4, P6, P8	Deaths, hospitalized, severely injured, moderately injured
P5	Deaths, critically injured, severely injured, moderately injured

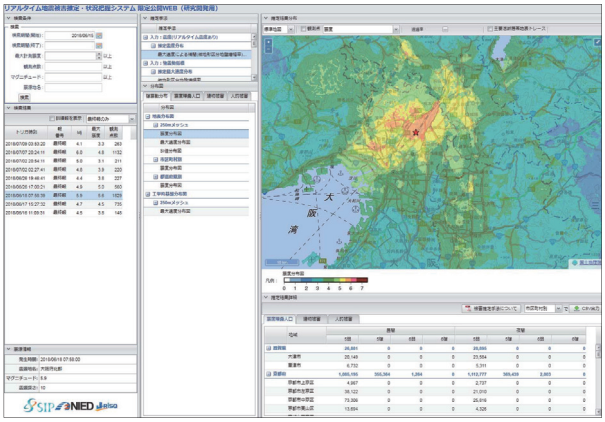

Fig. 4. Example of search results on the members-only website.

sure to seismic intensity, structural damage, casualties) or a prefectural or municipal thematic map. Further, a list of numerical data representing damage estimates organized by prefecture and municipality (e.g., population exposure to seismic intensity, structural damage, casualties) is displayed along with information related to the hypocenter and analysis conditions, and can be downloaded in CSV format.

For the general public, the website also releases the J-

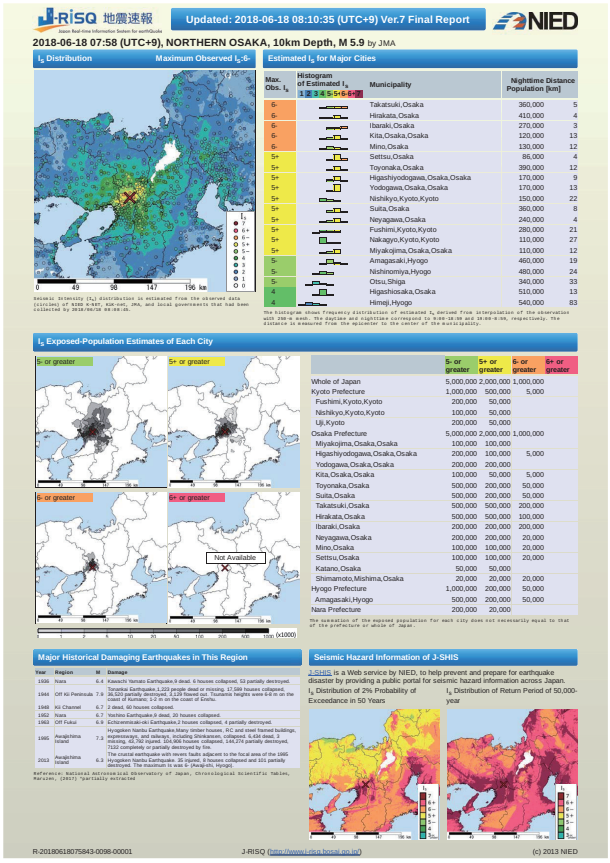

Fig. 5. Example of J-RISQ earthquake bulletin.

RISQ earthquake bulletin [17] that provides broad, easy-to-follow, and compact summaries of earthquake-related information using maps and tables, including seismic motion distributions and population exposure to seismic intensity estimated using a 250-m grid for each municipality. It also shows past earthquakes that caused damage in surrounding areas and information on earthquake hazards provided by J-SHIS (**Fig. 5**).

Damage estimates are intended to be used to make effective decisions related to emergency response immediately after a disaster strikes. The results are not only available for viewing using a browser but can be provided as numerical data for secondary use via a Web API, so that users can quickly utilize them in their own systems. A list of information available through the Web API is listed in **Table 6**.

2.6. Operation of the Real-Time Damage Estimation System

This section will outline how the system operated during actual earthquakes. In January 2016, the system began operating continuously on a trial basis after it was equipped with ground motion and structural damage estimation functions. **Table 7** shows a list of times from when the earthquake occurred until a final report was produced following earthquakes with a maximum seismic intensity of upper 5 or above between January 2016 and June 2018. Of the 22 earthquakes recording a seismic intensity of upper 5 or above during this period, the system estimated damage in 20 earthquakes. The results show that the system issued a final report no later than approximately 12 min after the earthquake occurred.

In addition, during the earthquake marked “Event 12,” one of the two earthquakes for which the system did not estimate damage, a seismic intensity of upper 5 was recorded only at one observation point and the earthquake involved a localized, intense ground motion immediately above the hypocenter. As a result, the number of observation points recording a seismic intensity of 2.5 or above did not exceed the threshold that triggers damage estimation in K-Net or KiK-net, and the system did not estimate damage. With respect to Event 4, Event 3 occurred approximately 2.5 minutes prior. The system therefore estimated the damage from Event 4 while processing Event 3 without making a distinction between the two earthquake events. It can be said that, since the system estimates damage based solely on ground motion observation data, instead of estimating the ground motion based on hypocenter data, its damage estimates are unlikely to be affected even in a case such as this when earthquakes occur virtually simultaneously.

Next, the system’s damage estimates for individual earthquakes will be discussed. Following the 2016 earthquakes in Kumamoto, the system completed estimation and dispatched a final report in roughly 10 minutes, after both the foreshocks and the mainshocks. As demonstrated by Fujiwara et al. [18], a comparison of the estimates with damage reports by local governments following the mainshocks and actual damage deciphered from aerial photos of buildings shows that the system’s evaluations of damage distribution, such as most damaged areas in Mashiki Town, Kumamoto Prefecture, were qualitatively consistent with the actual damage. At the same time, however, the system tended to overestimate the extent of damage in terms of quantity. A comparison of the number of completely destroyed buildings estimated by the system and the number deciphered from aerial photos is shown in **Fig. 6**. We are currently working to improve the damage estimation technique based on the actual damage data from the Kumamoto earthquakes [20].

The system completed estimating damage from the June 2018 earthquake in northern Osaka approximately 12 min after the earthquake, generating estimates on seismic intensity distribution and structural damage distribution shown in **Figs. 7** and **8**. This data was published on NIED’s crisis response site [21]. The estimated number of completely destroyed buildings varied significantly between 0 and 1,494 among the eight techniques shown in **Table 3**. Likewise, the estimated number of deaths due to structural damage varied from 16 to 76. According to the Fire Department, there were 18 completely destroyed residential buildings, 740 damaged non-residential buildings with unknown levels of damage, and six deaths [22]. Given that the technique that generated results that were closest to the actual damage (technique M8: 0 estimated completely destroyed buildings) used a damage function

Table 6. List of data available through Web API.

Category	Available data		Data format
Search	Published information (ID is obtained to access data)		JSON, CSV
Seismic ground motion	Ground surface (250-m grid)	Seismic intensity Peak ground velocity (PGV) Peak ground acceleration (PGA) SI values Velocity response spectra (Kanto and Tokai only)	netCDF(v4), CSV
	Engineering bedrock (250-m grid)	PGV PGA	
Population exposure to seismic intensity	250-m grid	Lower 5 or above, upper 5 or above Lower 6 or above, upper 6 or above	netCDF(v4), CSV
	By prefecture		JSON, CSV
	By municipality		JSON, CSV
Structural damage	250-m grid	Completely destroyed, partially destroyed	netCDF(v4), CSV
	By prefecture		JSON, CSV
	By municipality		JSON, CSV
Casualties	250-m grid	Deaths, critically injured, severely injured, moderately injured, evacuees	netCDF(v4), CSV
	By prefecture		JSON, CSV
	By municipality		JSON, CSV

Table 7. List of earthquakes detected by the system.

Event No.	Date and time of earthquake	Epicenter	Depth [km]	M	Maximum seismic intensity	Time between the earthquake and final report [s]
1	Apr. 14, 2016	Kumamoto area of Kumamoto Prefecture	11	6.5	7	542
2	Apr. 14, 2016	Kumamoto area of Kumamoto Prefecture	8	5.8	Lower 6	643
3	Apr. 15, 2016	Kumamoto area of Kumamoto Prefecture	7	6.4	Upper 6	639
4	Apr. 15, 2016	Kumamoto area of Kumamoto Prefecture	11	5.0	Upper 5	!]
5	Apr.16, 2016	Kumamoto area of Kumamoto Prefecture	12	7.3	7	604
6	Apr.16, 2016	Kumamoto area of Kumamoto Prefecture	11	5.9	Lower 6	398
7	Apr.16, 2016	Aso area of Kumamoto Prefecture	7	5.9	Upper 5	680
8	Apr.16, 2016	Aso area of Kumamoto Prefecture	11	5.8	Upper 6	211
9	Apr.16, 2016	Kumamoto area of Kumamoto Prefecture	16	5.4	Lower 6	628
10	Apr18, 2016	Aso area of Kumamoto Prefecture	9	5.8	Upper 5	648
11	Apr.19, 2016	Kumamoto area of Kumamoto Prefecture	10	5.5	Upper 5	633
12	Apr. 29, 2016	Central region of Oita Prefecture	7	4.5	Upper 5	!]
13	Jun. 16, 2016	Uchiura Bay	11	5.3	Lower 6	688
14	Oct. 21, 2016	Central region of Tottori Prefecture	11	6.6	Lower 6	726
15	Dec. 28, 2016	Northern region of Ibaraki Prefecture	11	6.3	Lower 6	643
16	Jun. 20, 2017	Bungo Channel	42	5.0	Upper 5	665
17	Jun. 25, 2017	Southern region of Nagano Prefecture	7	5.6	Upper 5	691
18	Jul. 11, 2017	Kagoshima Bay	10	5.3	Upper 5	679
19	Sep. 8, 2017	Southern interior of Akita Prefecture	9	5.2	Upper 5	648
20	Apr. 9, 2018	Western region of Shimane Prefecture	12	6.1	Upper 5	659
21	May 25, 2018	Northern region of Nagano Prefecture	6	5.2	Upper 5	652
22	Jun. 18, 2018	Northern region of Osaka Prefecture	13	6.1	Lower 6	721

whereby the ground motion inputs for wooden buildings were based on a velocity response spectrum with a period of 0.5 to 1.5 seconds (1 to 2 seconds for non-wooden buildings), estimates may have been based on seismic motion inputs with shorter predominant periods than the period bands described above. However, further analysis is needed.

2.7. Assessing Actual Damage

By employing damage functions to estimate damage, the system establishes a statistical relationship between ground motion intensity and damage levels based on past data such as earthquake damage surveys. Applying these statistics to actual earthquakes could potentially result in estimation errors. Meanwhile, efforts have been made to determine the extent of actual damage by analyzing satellite images, aerial photos, and images captured by dashboard cameras [23, 24]. Data on actual damage are highly accurate, but provide only fragments of information from both temporal and spatial standpoints, which is not necessarily effective for quickly grasping the overall damage after an earthquake. In order to quickly and accurately determine the extent of damage, we equipped the system with a technique for enhancing the accuracy of damage estimates over an extensive area by applying the Bayesian update to the damage estimates using information on actual damage obtained from some parts of the area [25].

In this technique, the structural damage function is defined as the probability distribution of seismic resistance, whereby the seismic resistance of buildings is expressed

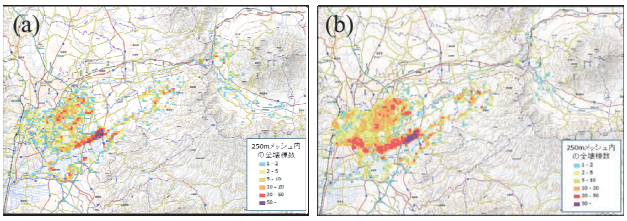

Fig. 6. A comparison of the distribution of completely destroyed buildings in the Kumamoto earthquakes: (a) damage distribution deciphered from aerial photos [19] and (b) an example of damage estimates (damage function: M1).

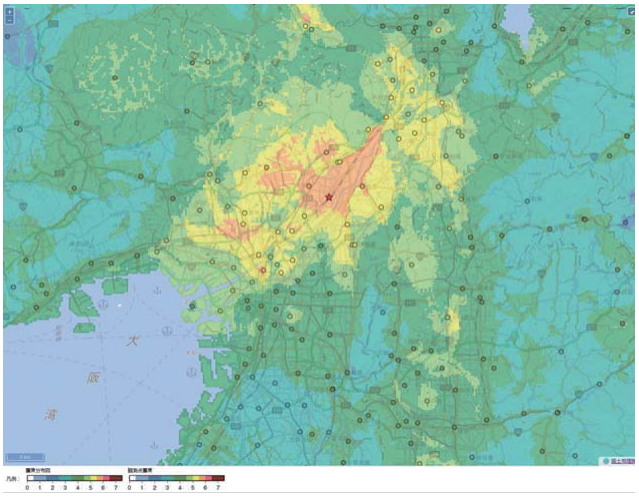

Fig. 7. Estimated distribution of seismic intensities in the earthquakes in Northern Osaka ("◯" represents an observation point and "☆" the epicenter).

in terms of ground motion intensity. The parameters of the damage function are then treated as probability variables. Information on actual damage is used as observation data input in the Bayesian update process. Then, the posterior probability distribution of the parameters of the damage function is obtained, and estimates are made with the updated parameters. By applying this update process each time data on actual damage are obtained, damage can be estimated on the basis of the latest data on actual damage.

The Bayesian update was applied to the estimates of damage to residential buildings caused by the 2016 Kumamoto earthquakes [26]. In this instance, a case study was conducted on areas that referred to data on actual damage to examine how damage estimates are updated. The study reported that by obtaining comparable data from Mashiki Town and Higashi-ku, Kumamoto City, respectively, and incorporating it into estimates, it is possible to improve estimates of the number of damaged buildings and bring them close to the actual number. Since estimation errors were not sufficiently improved in some areas, however, it has been suggested that methods used to gather information on actual damage should be studied in the future.

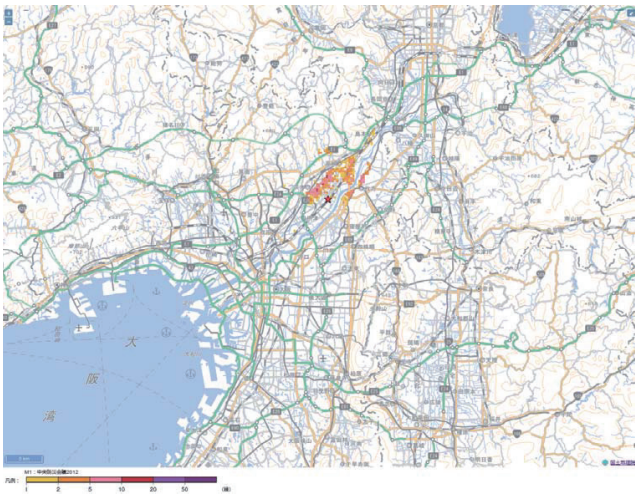

Fig. 8. Estimated distribution of buildings completely destroyed by earthquakes in Northern Osaka (example of estimates using estimation technique "M1").

2.8. Development of subsurface Structure Models for Estimating Earthquake Damage

To develop subsurface structure models for estimating earthquake damage on a real-time basis, we studied subsurface models capable of evaluating ground motion characteristics at a broad range of frequencies (0.1 Hz to 10 Hz). We combined a shallow subsurface model and a deep subsurface model by collecting boring data and soil property data, which are crucial for explaining the ground motion in the vicinity of each period (0.5 to 2.0 s), as such ground motion affects soil both near the surface and deep in the ground. In this study, we developed a wide-area subsurface structure model (approx. 250-m grid cell) and a more detailed subsurface model (approx. 50-m grid cell), as well as a microtremor measurement system and a subsurface structure information management system to support model development.

A brief description of each of the following themes will be provided in the sections below.

(1) Construction of wide-area subsurface models for estimating earthquake damage

(2) Understanding of ground motion characteristics and development of a microtremor observation system

(3) Development of a construction technique for a detailed subsurface model through public-private collaboration

2.8.1. Construction of Wide-Area Subsurface Models for Estimating Earthquake Damage

Wide-area subsurface models were constructed for the entire Kanto and Tokai regions. Here, we will mainly report on the progress made with the model for the Kanto area. To develop a shallow subsurface model, we primarily used approximately 31,000 sets of boring data gathered by NIED. An initial shallow subsurface model was

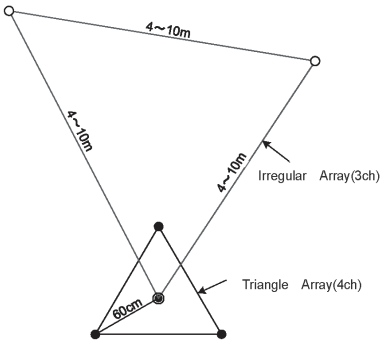

Fig. 9. Conceptual diagram of miniature and irregular seismic arrays.

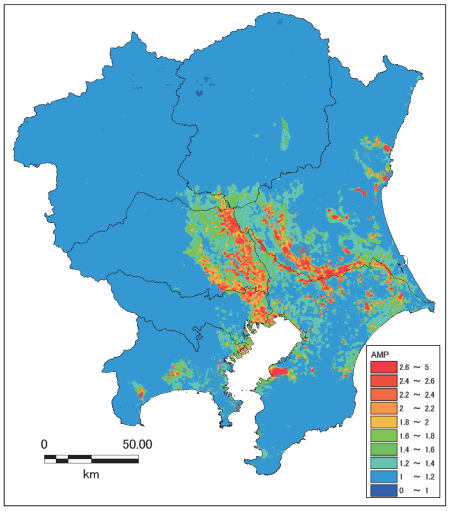

Fig. 10. One-dimensional S-wave amplication factor from basement (Vs400 m/s) to surface at period 1 s in Kanto area.

constructed by reorganizing existing models, including a shallow subsurface model for the Kanto region [27] and subsurface models prepared thereafter by local governments, so as to sort data on subsurface rock and soil strata across the entire Kanto region in a unified manner. We created an initial integrated model for shallow and deep subsurfaces by combining this shallow subsurface model with an existing deep subsurface model (J-SHIS) and adjusting the engineering bedrock (Vs = 300 to 700 m/s). In addition, seismic observation records and continuous microtremor observation data were gathered to conduct a 3-D study of S-wave velocity structures, which are essential for evaluating ground motion. Records compiled by K-NET, KiK-net, JMA, and local governments were used as seismic observation records. To gather continuous microtremor data, two types of observation techniques, namely miniature and irregular arrays [28] (**Fig. 9**) and large arrays (R = 25 to 800 m), were used at approximately 14,000 and 500 points, respectively. Microtremors were observed using single-point and miniature arrays at intervals of approximately 1 to 2 km for 15 min each time. Observations using large arrays were conducted at intervals of approximately 5 km for 1 to 2 h each time. In analyzing miniature and irregular arrays, we used a cloud microtremor observation system (described in Section 2.8.2) and other systems to derive the H/V spectral ratio and phase velocity. Depth conversion (SPM) [29] and inversion analysis [30] were carried out on the dispersion curve to obtain S-wave velocity structures. By fine-tuning the S-wave velocity structures of the initial model, we calculated amplification indicators (e.g., peak velocity amplification factor, seismic intensity increment, response amplification factor for each period) based on the subsurface structure models for each grid cell of approximately 250 m by 250 m. (**Fig. 10**). A comparison of the new model against the existing subsurface model shows that improvements have been made in the estimates of period characteristics across all frequencies.

2.8.2. Understanding Ground Motion Characteristics and Development of a Microtremor Observation System

To obtain a large number of microtremor array measurements and ensure that results are managed effectively until the results of analysis are produced, it is necessary to minimize and simplify the steps required to collect observation data, analyze them, and evaluate the results. Particularly from the time observation data are gathered until it is analyzed, a significant amount of time is required to check data, convert data formats, sort photos, and complete other sorting required for analysis. To achieve these goals, we developed a mechanism that can perform all the steps quickly, including on-site data sorting and analysis (registering data such as location information, photo information, observation data, time-history data, and analysis results) while minimizing human error [31]. More specifically, we developed "i-Bido" [32], which transmits data between seismometers and computers, tablets, and other computing devices without corrupting the data while preserving its quality, and sends the data to the database described below. Data registered in the database is automatically managed for quality assurance and analyzed. Then, the S-wave velocity structures obtained from the analysis (subsurface models), along with mapping information, need to be distributed and confirmed using WebGIS or other means on a virtually real-time basis. To this end we developed a cloud analysis system that analyzes and tests the quality of microtremor data at high speed. The system structure and a conceptual diagram are shown in **Fig. 11**. In cloud analysis, the input data are analyzed in detail and managed for quality assurance. When our cloud system is used, the steps between observation and analysis are completed roughly five to ten times faster than when the system is not used.

2.8.3. Development of a Construction Technique for a Detailed Subsurface Model Through Public-Private Collaboration

Our goal is to construct detailed subsurface models with 50-m grid cells capable of predicting liquefaction and landslides while accounting for factors such as ground

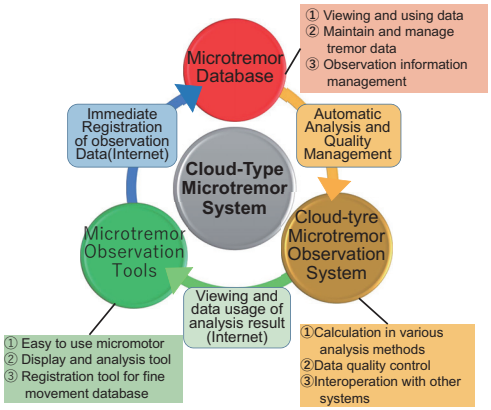

Fig. 11. Development of cloud-type microtremor observation system.

irregularity and artificial sites, using both public and private boring data, building confirmation applications, topographical information, old topographic maps, and other data. A slope map developed by the Geospatial Information Authority of Japan (GSI) for a study of artificial sites in Yokohama City indicates horizontal surfaces in white and sloped (inclined) surfaces in gray, with larger angles of slope shown in darker gray. Angles of slope (inclination) between 0° (horizontal) and 1° are indicated in gray, while those of 10° or above are shown in black. Man-made structures were excluded. The distribution of small artificial valley fills that could not be identified by topographical maps derived from an algorithm for calculating and comparing slopes was obtained. Finally, the buffer region (50 m per side at a zero-order basin, 37.5 m per side for a one-order valley, and 25 m per side for a two-order valley) was applied to the water systems identified from the results of water system analysis to develop a model. The model is consistent with the distribution of large-scale artificial sites and also appears to show small artificial sites (**Fig. 12**).

3. Development of High-Resolution Damage Estimation Technology Using Structural Analysis

While earthquake response analysis is used to design earthquake-resistant buildings, techniques for estimating earthquake damage in urban areas rely largely on empirical equations that are not computationally demanding and require a small amount of input, given the large number of building structures subject to computation. Meanwhile, the amount of usable information on urban areas has grown dramatically, and significant improvements have been made in computational methods and the technologies for applying such methods. In this section we will describe our technical development efforts aimed at establishing a method for estimating earthquake damage using simulations based on detailed information related to urban areas.

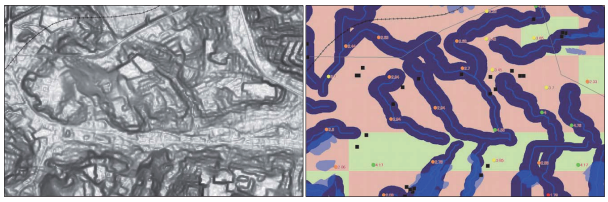

Fig. 12. Distribution of artificial sites extracted from the slope map (left figure) based on the 5mDEM data of the Geographical Survey Institute of Japan in Yokohama City. Right figure is the range of the extracted area where the indigo is extracted, light purple is the past large scale area distribution map.

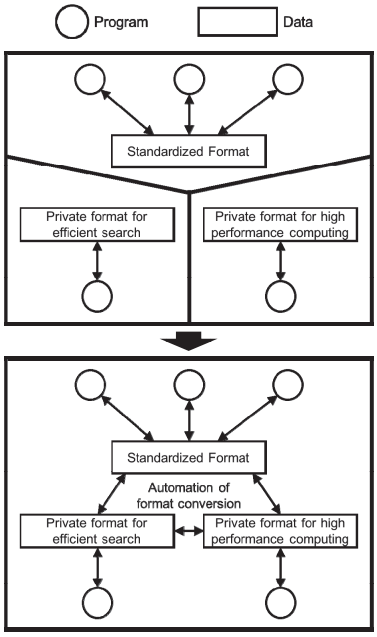

Fig. 13. A solution to data silo problem.

3.1. Development of a Data Processing Platform

Exponential improvements are already being made to computational techniques and application software in the field of high-performance computing (HPC). In this study, we therefore focused on technical development for automatically constructing the city models that serve as input for clusters of analysis programs capable of performing large-scale numerical analysis, and technologies that link the analysis programs with one another. A common issue encountered in developing city models is that data on urban areas, which are used to construct city models, and analysis programs are evolving constantly, and it is not easy to respond quickly and flexibly to new data and programs. To solve this problem, we developed a data processing platform (DPP) capable of connecting data programs while allowing users to easily add and replace data and programs. The most characteristic feature of DPP is that it is based on a new methodology, whereby a structure, or a data format, is automatically converted into a different but logically equivalent one (**Fig. 13**). Such an

automatic conversion function is particularly essential in HPC, where enhancing computational efficiency and conserving memory capacity are some of the most important goals. Generally speaking, data are shared in formats specified by the International Organization for Standardization (ISO), and in most cases human-readable text formats are used. In HPC, however, binary formats are normally used, and efforts are made to put the same type of data in a single line so that all the data can be processed at high speed. In addition, data searches are normally performed by accessing a portion of the data. For this reason it is important to structure the data into groups of similar meaning or subject content to search. Even if data have similar meanings or content, it is defined by a broad range of formats based on a diverse range of data processing objectives by those performing computation or managing data. To make data available for secondary applications and link it with other data, therefore, it is necessary to first study individual data formats and create data processing programs for each format, even if they are identical in nature. By automatically converting data formats, the DPP eliminates the need to create a data processing program for each data format and thus is able to standardize all data formats so that a processing program developed for one data format can be applied to all data with equivalent meaning or content. This function allows for connection and interaction between independently developed clusters of individual data formats and processing programs unique to them (**Fig. 13**). The outstanding reusability of programs used on the DPP helps users build up component technologies needed to automatically construct a city model using a diverse range of digital data on urban areas. Right from the start, it is important to employ a design that prevents technology development from stagnating by avoiding overlaps in development. This study has confirmed that it is possible to create modules for automatically creating models for soil, buildings, and various types of critical infrastructure [33, 34] as a library of DPP, which interprets and automatically converts data. This computation can be performed by a program developed by HPC.

3.2. Construction of Simulated City Models for Cities Across Japan and Automated Performance of Earthquake Response Analysis

To automatically estimate damage after an earthquake, city models covering all areas of Japan must be constructed in advance. In this study, the DPP was made into a parallel program using the message passing interface (MPI), making it possible to construct models for approximately 60 million structures across Japan in roughly six hours (**Fig. 14**). However, since data generated by an inexpensive residential map (Zenrin Zmap-AREA II) were used, hypothetical values had to be set for building heights. By expanding the functionality of the DPP to enable automatic analysis of earthquake response, it is now possible to generate earthquake response analysis with consistent quality by providing the DPP with data on structural height, ground motion, and soil.

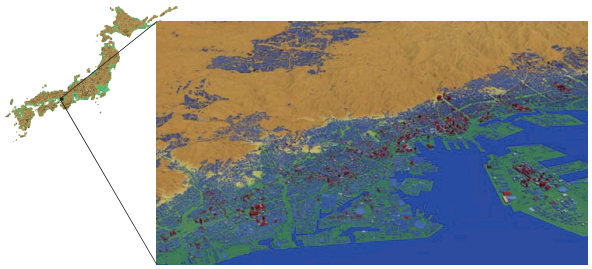

Fig. 14. Automatic construction of building models for the whole Japan.

3.3. Future Outlook

In the field of HPC, the development of a system capable of making comprehensive predictions on compounding disaster risks is currently underway. The high reusability of programs enabled by the DPP helps the system achieve continuous expansion and upgrades. The system is expected to make significant contributions to the overall advancement of disaster prevention and mitigation efforts.

4. Research and Development Related to Disaster Information Extraction Using Earth Observation Satellites

4.1. Characteristics of ALOS-2

Equipped with PALSAR-2, an L-band synthetic-aperture radar (SAR), ALOS-2 can monitor the earth's land surfaces at any time of day or night and in any weather condition, in addition to offering the global observation, broad and periodic coverage, and disaster resistance that are the hallmarks of satellites. In addition, ALOS-2 can observe Japan and surrounding areas up to twice a day. The exterior and primary characteristics of ALOS-2 are shown in **Fig. 15** and **Table 8**, respectively.

These features make ALOS-2 particularly effective in capturing inundated areas following windstorms, floods, tsunamis, earthquakes, and gathering other disaster-related information. Because of space limitations, this section will focus on torrential rain, which has been occurring in Japan almost every year during the last few years, to discuss the flooded areas identified by ALOS-2 and how the results are being utilized at disaster sites.

4.2. Flooded Areas Identified by ALOS-2 and On-Site Application of Data

Results obtained by ALOS-2 were used to conduct a detailed study on actual disasters, including the flooding in Joso (Ibaraki) resulting from the torrential rains in the Kanto and Tohoku areas in September 2015, Typhoon Lionrock and the torrential rains in Hokkaido in August

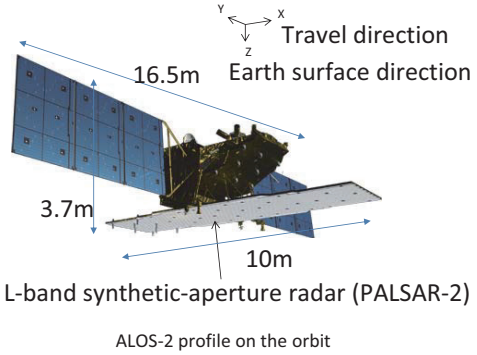

Fig. 15. Exterior of ALOS-2 in orbit.

Table 8. Primary characteristics of ALOS-2.

Orbit	Type	Sun-synchronous sub-recurrent orbit (with a revisit cycle of 14 days)
	Altitude	628 km (over the equator)
	Local sun time	12:00 (noon) over the equator (at descending node)
Design life		5 years (target: 7 years)
Launch date		May 24, 2014
SAR frequency		L-band (1.2 GHz band)
Primary observation modes	High-resolution	Resolution: 3/6/10 m Observation width: 50/50/70 km
	Wide-area observation	Resolution: 100/60 m Observation width: 350/490 km

2016, the heavy rainfalls in northern Kyushu in July 2017, and the torrential rainfalls in western Japan in 2018. Here, we will discuss the flooding of the Omoto River caused by Typhoon Lionrock that resulted in a large number of casualties.

After receiving an emergency observation request from the Ministry of Land, Infrastructure, Transport and Tourism (MLIT), ALOS-2 observed the shorelines of Iwate Prefecture on August 30 at 22:43 and submitted the identified flooded areas to the MLIT the next morning. **Fig. 16** shows the results generated by ALOS-2 and the actual flooded areas [35]. Overall, the results are consistent with each other.

The data provided by ALOS-2 was used by the MLIT to develop a helicopter route for conducting a disaster-preparedness survey.

4.3. Summary

Information related to flooded areas and areas with structural damage identified using ALOS-2 observation images is linked to the real-time damage estimation, and application system developed by NIED [36] and disaster information systems operated by disaster management

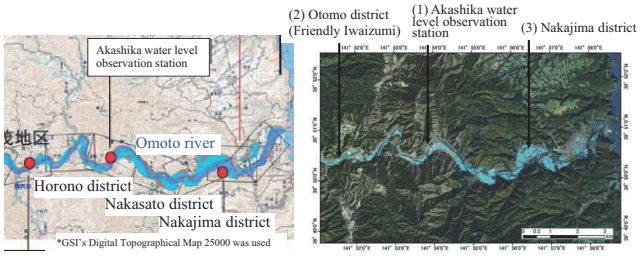

Fig. 16. Flooded areas identified by ALOS-2 (right) and a map showing actual flooded areas.

institutions via the ALOS-2 disaster information product processing system. This allows users to use the data in their own systems for disaster management and helps identify the extent of damage more quickly.

5. Development of Disaster Information Summarization System Using Social Media

The National Institute of Information and Communication Technology (NICT) has developed "D-SUMM," a disaster information summarization system which summarizes the disaster reports from a specified area in a compact format and enables rescue workers to quickly grasp the situation. D-SUMM has been released on a trial basis since 2016. This system was used in the disasters induced by heavy rainfalls in Northern Kyushu in 2017.

5.1. Development of D-SUMM

One of the lessons we learned from the 2011 Great East Japan Earthquake was that a large-scale disaster can destroy infrastructure, disrupt lives, and cause many unpredictable situations. Immediately after the disaster, massive amounts of useful information filled the internet, especially through social media platforms such as Twitter. Nevertheless, because most people were overwhelmed by the huge amount of information, they were unable to make appropriate decisions and much confusion ensued.

In September 2015, an initiative called "Resilient Disaster Reduction and Mitigation" (managed by the Japan Science and Technology Agency (JST)), was launched through the Cross-ministerial Strategic Innovation Promotion Program (SIP), a program spearheaded by the Council for Science, Technology, and Innovation of the Cabinet Office. Under this initiative the development of a disaster information summarization system called D-SUMM began. D-SUMM automatically extracts disaster reports from tweets from specified areas (prefecture or municipality) and time periods to summarize them. The development of D-SUMM greatly enhanced a semantic-classification dictionary containing 28 million words called *Disaster Ontology*. Initially, *Disaster Ontology* contained 70 semantic categories in a single layer. This structure was modified into a two-layer structure by

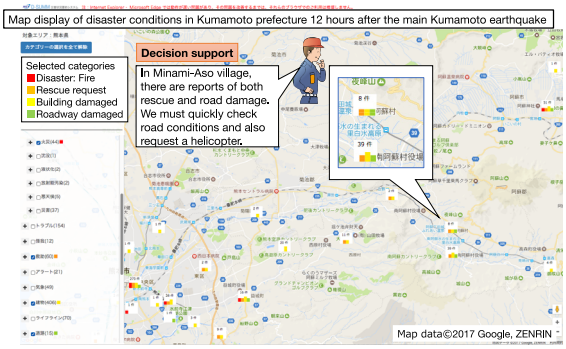

Fig. 17. Example of a D-SUMM map display (trial version for Kumamoto Earthquakes in Japanese).

creating an average of 11 semantic categories (subcategories) under each of these 70 categories.

Although we created two layers of semantic categories, not all words were properly classified into these categories. A special category called "unclassified" was created in the second layer, and most of the words were initially classified into this special category. Currently, 2.4 million words, which are considered particularly relevant in a disaster situation, are assigned appropriate labels in the second layer. By combining *Disaster Ontology* with other dictionaries that we have created, we have completed D-SUMM, the world's first system that automatically extracts disaster reports from Twitter and organizes, summarizes, and presents the content in a user-friendly way. D-SUMM gathers reports that use similar expressions and summarizes them into a single report to present a more compact output. By producing summaries of disaster reports for each of the sub-areas comprising a specified area (e.g., municipalities of Kumamoto Prefecture if Kumamoto Prefecture is specified), this function enables users to quickly understand what is happening in which sub-area. Multiple categories can also be specified and displayed on a map, along with the number of times an item has been reported, making it easy to gain an overview of disaster conditions on the map (**Fig. 17**).

5.2. Practical Application of D-SUMM

In January 2017, D-SUMM was incorporated into disaster simulation drills conducted by the Tokyo Metropolitan Government. 7,000 social media posts were prepared on the basis of the scenario of a massive earthquake striking Tokyo to simulate a realistic situation for the drills. An employee of the Tokyo Metropolitan Government who participated in the drills said, "We realized that social media posts serve as important sources of information for understanding what's going on right after the disaster." Another commented that "local government officials must be able to use such systems in the future."

In April 2017, D-SUMM was also used in disaster simulation drills conducted by the Oita Prefectural Government. We prepared 5,800 posts for the disaster simulation drills based on the assumption that a Nankai Trough earthquake had just occurred. In addition, during the disasters induced by heavy rainfalls in Northern Kyushu in July 2017, D-SUMM was used by the Oita Prefectural Government. As a result, it was possible to quickly gather disaster information. For example, the fact that a railway bridge was washed away was discovered using social media posts earlier than Kyushu Railway Company did. A person in charge commented that "the system was useful because a wide range of information came from victims."

D-SUMM has been used not only in natural disaster exercises, but also in a civil protection simulation drill. In January 2018, the Iwate Prefectural Government used our system in a civil protection simulation drill based on the scenario that a terrorist attack occurred during an international friendly rugby match during the Rugby World Cup 2019. This was the first attempt to use D-SUMM for a civil protection simulation drill. We fine-tuned the system so that terms and expressions related to terrorist attacks will be handled properly. The drill was a great success, and the systems received high marks for being particularly effective, especially amid the confusion immediately after the first attack.

Meanwhile, social media has caused confusion following some natural disasters. During the heavy rainfalls in July 2018, for example, "#rescue" was used in unintended ways on Twitter. Further, false rumors spread on Twitter and LINE following the 2018 Hokkaido Eastern Iburi Earthquake. Efforts to advance the technologies discussed in this section and to promote their widespread application through repeated demonstration experiments must be made to mitigate the confusion brought on by social media. In addition, improving the literacy of both providers and recipients of information on social media is crucial to enhance its applicability in disaster situations.

6. Development of Real-Time Monitoring Technology for Volcanic Gases and Ash

In this project, we developed devices and systems that automatically take measurements, transfer data, conduct initial analyses on, and publish volcanic gas emission rates, volcanic gas composition, and volcanic ash images to allow users to grasp volcanic activities quickly and accurately. The application of the devices made it possible to quickly grasp the activities of Shinmoedake and Iwoyama volcanoes, which are part of Kirishima volcanoes, just before they erupted in March and April 2018.

Volcanic gas emission rates change when magma rises from the volcano and magmatic gases interact with hydrothermal systems. Emission of sulfur dioxide, in particular, suggests the involvement of magma. Monitoring sulfur dioxide emission rates is therefore essential to understanding volcanic activities. In this project, we developed a zenith sky SO_2 monitoring device (**Fig. 18(a)**) and studied a technique for monitoring the emission rates of sulfur dioxide on a real-time basis by installing the devices and taking measurements at multiple locations. To demonstrate the validity of this technique, we constructed

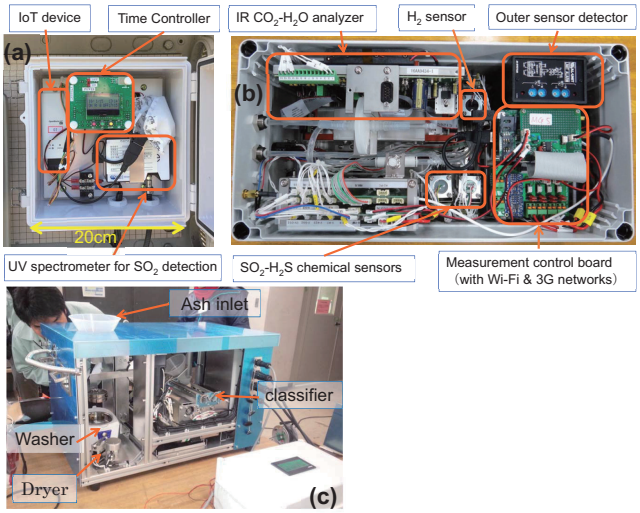

Fig. 18. (a) A main part of zenith sky SO_2 monitoring device used for SO_2 flux monitoring network. (b) Multi-GAS for volcanic gas composition measurement. (c) VOLCAT (Visual Observation Laboratory Capturing Ash Transition) for on-site imaging of ash particles.

and operated an observation network in the southeastern region of Sakurajima consisting of sites where the newly developed devices were installed. In Sakurajima, we are working to enhance our analysis technique while operating our observation network so as to be able to obtain reliable measurements of sulfur dioxide emission rates more frequently. In October 2017, the Shinmoedake volcano erupted for the first time in six years. Following the eruption, we installed our zenith sky SO_2 monitoring devices at three locations and began monitoring the volcano in November 2017. While it is difficult to quantify sulfur dioxide emission rates by relying on measurements from only these three locations, it is possible to monitor changes in emission rates qualitatively. On March 1, 2018, an even larger eruption occurred at Shinmoedake, roughly four and a half months after the eruption in 2017. The monitoring conducted as part of this project suggested the possibility that gas emissions began to intensify about a week before the March 1 eruption. Further, this project revealed that Shinmoedake was emitting a large amount of volcanic gases, in accordance with increasing levels of volcanic tremors, on March 1 before the eruption was confirmed by ash fall.

Measuring volcanic gas composition is useful for capturing changes in volcanic activities, since the composition fluctuates according to changes in the temperatures and pressures of magma and hydrothermal systems. In the past, however, observation was not conducted frequently since samples had to be taken directly for analysis. Further, analysis required a great deal of time. In this project, by upgrading a multicomponent gas analyzer system (Multi-GAS) that automatically measures volcanic gas composition, we developed a system capable of automatically taking repeated measurements of volcanic gas, transferring measurement data, and conducting initial analysis (**Fig. 18(b)**). The Multi-GAS was installed and currently operates at Sakurajima, which is erupting regularly, as well as at Shinmoedake and Iwoyama, where activity has increased. We began observing Iwoyama in July 2017, because of increasing fumarolic activity since 2016. Our observation revealed that, two to three months before the eruption of Iwoyama on April 19, 2018, the SO_2/H_2S molar ratio in its volcanic gases increased from 0.01 to roughly 1. By measuring such abrupt changes in volcanic gas composition in real time, the device will likely make it possible to quickly assess the possibility of volcanic eruption.

Volcanic ash has been used to grasp changes in volcanic activities since its composition reflects the type of volcanic eruption and samples can be collected relatively safe. However, since volcanic ash observation was conducted in laboratories in the past, it took at least half a day to collect samples on site and transmit observation data. We developed a portable automated volcanic ash sampling and analysis device, or Visual Observation Laboratory for Capturing Ash Transition ("VOLCAT"; **Fig. 18(c)**), with the goal of expediting volcanic ash observation and data transmission. This device, when installed in ash fall areas, can automatically sample, clean, dry, classify, and capture microscopic images of volcanic ash, and transmit data to a specified server within set time intervals. In response to the eruption activities of the Shinmoedake volcano, which has been active since October 2017, we installed VOLCAT at NIED's V-net Hinamoridai observation point at Kirishima volcano and began monitoring volcanic ash. From our observations we were able to capture microscopic images of volcanic ash generated by the eruptions of Shinmoedake that occurred between March 13 and 15 in 2018. The images of the volcanic ash we obtained largely consisted of angular particles ranging in color from black to paler colors, resembling the volcanic ash generated by Vulcanian eruptions, which explode shattered crystalized lava domes accumulated in shallow conduit regions. VOLCAT has the potential to become a new tool for quickly capturing changes in eruption activities.

We also developed an information platform for compiling data obtained using the various monitoring devices and displaying them on websites through data application systems for disaster response support [36]. This platform aids creating an environment for helping both central and local governments to obtain information on volcanic activities quickly and to make effective decisions based on the observation data and advice of researchers. Further, we developed a trial version of a volcanic disaster survey support function for quickly gathering updates on ash falls and other volcanic activities, likewise contributing to an environment where information can be shared. Data obtained using observation devices installed at Sakurajima and Kirishima volcanoes are shared virtually in real time with researchers, JMA, local governments, and others working in volcanic disaster prevention.

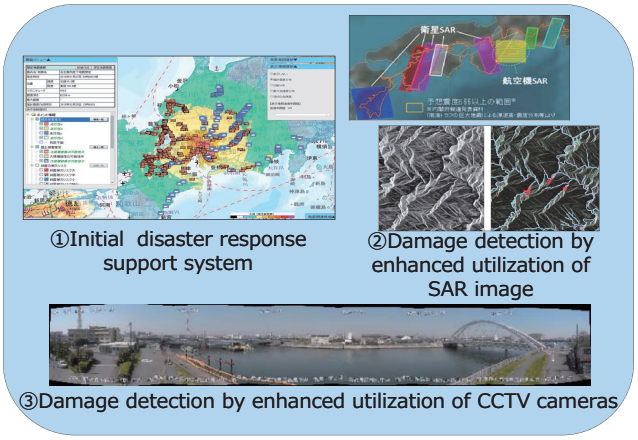

Fig. 19. Development of technology for Infrastructure Damage Detection.

7. Development of Real-Time Collection, Integration, and Sharing Technology for Infrastructure Damage Information

At the time of occurrence of a disaster, the officials of the Regional Development Bureaus, and so on, who are engaged in disaster-response activities, are required to establish initial disaster response system and take appropriate decisions based on the limited information and the situation changing moment by moment.

To address this problem, "a real-time collection, integration, and sharing technology for infrastructure damage information" has been developed aiming to support decision making based on the chronological passage of the disaster and implement a suitable system for the initial response, such as emergency lifesaving work (**Fig. 19**). This technology has been steadily implemented and applied to provide information for officials in charge of disaster response during torrential rains or earthquakes. To promote technological development based on the information needs on the site of disaster response. Interview surveys were conducted in order to clarify the information needs in the case of the 2016 Kumamoto Earthquakes. While the information needs are arranged along the time axis, the method is expected to evaluate the current situation of technology to grasp infrastructure damage information based on the three indices of "promptness," "coverage," and "reliability" in this survey. Please refer to the literature [37] printed in this issue of JDR for details.

8. Conclusion

We developed a real-time damage estimation system with the aim of helping organizations establish a first response system as quickly as possible in the event of earthquakes and other natural disasters. With respect to real-time damage estimation, the system is able to predict the distribution of strong ground motion, structural damage, and casualties, displaying the data on the website in roughly 10 minutes after a major earthquake, while outputting digital data in a reusable format. With regard to damage estimation, we developed a system that assesses damage by identifying damage over an extensive area through satellite image analysis, summarizing disaster information based on social media posts and utilization of CCTV cameras or SAR images among other methods. These systems were used for disaster response during the 2016 Kumamoto earthquakes, and demonstrated their effectiveness. In addition, a system was developed to monitor volcanic gases and ash for volcanic eruptions, now installed at Sakurajima and Mt. Kirishima.

While the spatial distribution of damage from the Kumamoto earthquakes estimated by the damage estimation system was qualitatively consistent with the actual damage, the system tended to overestimate the extent of damage in terms of quantity. Potential future topics of study include making improvements to the system's tendency to overestimate the number of damaged buildings and showing the results of estimation as values with a certain width. Another goal is to further develop the system so that it can connect and integrate damage estimates more organically, and information on actual damage can be identified through various means while sending necessary information to institutions as needed.

One of the biggest goals of SIP is social implementation of research outcomes. Throughout our research and development projects we encouraged private corporations, local governments, and other institutions to make use of our real-time damage estimates and information on actual damage in disaster response, business continuity planning, and disaster management business. As part of our efforts, we have launched a hazard risk experiment consortium and are developing a mechanism through which we can share damage estimates with participating institutions, so that they can respectively make use of the information according to their needs. Through this initiative, we are studying a framework for the full-scale implementation of the system, identifying issues, and discussing possible solutions.

We will continue to further enhance and implement the system in collaboration with the affiliated institutions so that our real-time damage estimation system can be used effectively in responding to earthquake, tsunami, and heavy rainfall disasters caused by major earthquakes such as the Nankai Trough earthquakes and massive earthquakes in Tokyo that are believed likely to happen in the future. At the same time, we will need to examine how to develop a framework that enables stable operation and management of the system, which is one of our biggest challenges for the future.

Acknowledgements

This study was supported by Council for Science, Technology and Innovation (CSTI), Cross-ministerial Strategic Innovation Promotion Program (SIP), "Resilient Disaster Reduction and Mitigation" (Funding agency: Japan Science and Technology Agency (JST)).

Data used by the real-time earthquake damage estimation system was recorded by local governments and the JMA, and provided by the JMA.

References:

[1] H. Nakamura, S. Aoi, T. Kunugi, W. Suzuki, and H. Fujiwara, "Prototype of a Real-Time System for Earthquake Damage Estimation in Japan," J. Disaster Res., Vol.8, No.5, pp. 981-989, 2013.

[2] National Research Institute for Earth Science and Disaster Resilience, "J-SHIS (Japan Seismic Hazard Information Station)," http://www.j-shis.bosai.go.jp/ [accessed July 16, 2018]

[3] S. Senna, A. Wakai, K. Jin, T. Maeda, and H. Fujiwara, "Modeling of the subsurface structure from the seismic bedrock to the ground surface for a broadband strong motion evaluation in Kanto Area, Japan," 16th World Conf. on Earthquake Engineering, Santiago, 2017.

[4] M. Ooi, K. Ishibashi, and H. Fujiwara, "Development of the building structure database for seismic risk evaluation," Proc. of the 13th Japan Earthquake Engineering Symp., pp. 1708-1715, 2010 (in Japanese with English abstract).

[5] Central Disaster Management Council, "Outline of damage estimation items and estimation methods of building damage and causalities by the Nankai Trough Big Earthquake," http://www.bousai.go.jp/jishin/nankai/taisaku_wg/pdf/20120829_gaiyou.pdf, 2012 (in Japanese) [accessed July 16, 2018]

[6] K. Horie, "Story collapse damage of wooden buildings by Great Hanshin-Awaji Earthquake," Earthquake J., No.38, pp. 30-40, 2004 (in Japanese).

[7] O. Murao and F.Yamazaki, "Building Fragility Curves for the 1995 Hyogoken-nanbu Earthquake Based on CPIJ & AIJ's Survey Results with Detailed Inventory," J. Struct. Constr. Eng. (Trans. of AIJ), No.555, pp. 185-196, 2002 (in Japanese with English abstract).

[8] O. Murao and F. Yamazaki, "Development of Fragility Curves for Buildings Based on Damage Survey Data of a Local Government after the 1995 Hyogoken-nanbu Earthquake," J. Struct. Constr. Eng. (Trans. of AIJ), No.527, pp. 189-196, 2000 (in Japanese with English abstract).

[9] Central Disaster Management Council, "Damage estimation method from Tokyo Inland Earthquake," http://www.bousai.go.jp/jishin/syuto/pdf/shiryou3.pdf 2004 (in Japanese) [accessed July 16, 2018]

[10] T. Takuma, I. Takahashi, H. Fujiwara, and Y. Kunimatsu, "Development of damage ratio curves for wooden buildings taking into account period characteristics," Summaries of Technical Papers of Annual Meeting, Structure-II, pp. 19-20, 2016 (in Japanese).

[11] S. Midorikawa, Y. Ito, and H. Miura, "Vulnerability Functions of Buildings based on Damage Survey Data of Earthquakes after the 1995 Kobe Earthquake," J. of JAEE, No.11, No.4, pp. 34-47, 2011 (in Japanese with English abstract).

[12] S. Shimizu, H. Fujiwara, H. Nakamura, N. Morikawa, T. Saeki, Y. Komaru, M. Wakaura, Y. Tokizane, and Y. Hayakawa, "Study of the Fragility Function of the Response Spectrum based on the definition of disaster victim certificate," Proc. of the Annual Conf. of the Institute of Social Safety Science, No.39, 2016 (in Japanese with English abstract).

[13] Kyouikusolution Corporation, "National school data (2015 version)," 2015.

[14] Agoop Corp., "Point-type floating population data," 2015.

[15] T. Takuma, M. Nakamura, T. Watanabe, and S. Midorikawa, "A Method for Quantitative Evaluation of Casualties and Medical Cost Assessment in case of an Earthquake," Proc. of Institute of Social Safety Science, No.3, pp. 133-140, 2001 (in Japanese with English abstract).

[16] S. Okada and T. Nakashima, "A New Causality Model for Evaluating the Probability of Human Damage from Injury to Death Associated with Building Collapse," Health and Labor Sciences Research Grant Report, pp. 147-161, 2015 (in Japanese).

[17] National Research Institute for Earth Science and Disaster Resilience, "Report of J-RISQ (Japan Real-time Information System for Earthquake)," http://www.j-risq.bosai.go.jp/report/ [accessed July 16, 2018]

[18] H. Fujiwara, "Development of real-time earthquake damage information system," Proc. of 13th JAEE Annual Meeting, A-4, 2017 (in Japanese).

[19] N. Monna, H. Fujiwara, H. Nakamura, T. Saeki, H. Shimomura, T. Yamada, and S. Fujisawa, "Feature of the building damage of Kumamoto earthquake by airphoto-interpretation," Japan Geoscience Union Meeting, HCG37-P10, 2017.

[20] N. Monna, H. Fujiwara, H. Nakamura, S. Naito, H. Shimomura, and T. Yamada, "Construction of earthquake building damage information space database and examination of building damage curve," The 15th Japan Earthquake Engineering Symp., PS1-01-33, 2018 (in Japanese with English abstract).

[21] National Research Institute for Earth Science and Disaster Resilience, "Crisis Response Site (The Earthquake in Osaka-Fu Hokubu)," http://crs.bosai.go.jp/DynamicCRS/index.html?appid=7f61007cafa949708cd5471bc6c52188, 2018 [accessed July 16, 2018]

[22] Fire and Disaster Management Agencyof the Ministry of Internal Affairs and Communications, "Damage by The Earthquake in Osaka-Fu Hokubu and Measures Taken by Firefighting Organizations ect. (Report No.30, 2018.11.6)," http://www.fdma.go.jp/bn/2018/detail/1050.html (in Japanese) [accessed December 11, 2018]

[23] R. Natsuaki, H. Nagai, N. Tomii, and T. Tadono, "Sensitivity and Limitation in Damage Detection for Individual Buildings Using InSAR Coherence.A Case Study in 2016 Kumamoto Earthquakes," Remote Sens., Vol.10, Article No.245, doi:10.3390/rs10020245, 2018.

[24] S. Naito, H. Tomozawa, Y. Mori, T. Nagata, K. Mitsuhashi, T. Yamada, H. Shimomura, N. Monna, H. Nakamura, and H. Fujiwara, "Development of the damage detection method for buildings with machine learning techniques utilizing aerial photographs of the Kumamoto earthquake," Japan Geoscience Union Meeting, SSS14-04, 2018.

[25] A. Kusaka, H. Nakamura, H. Fujiwara, and H.Okano, "Bayesian Updating of Damaged Building Distribution in Post-Earthquake Assessment," J. of JAEE, No.17, pp. 16-29, 2017 (in Japanese with English abstract).

[26] A. Kusaka, H. Nakamura, H. Fujiwara, K. Kanda, and N. Monna, "Estimation of damaged house distributions by use of aerial photographs of disaster area by the 2016 Kumamoto earthquake," Proc. of 13th JAEE Annual Meeting, P1-34, 2017.

[27] S. Senna, T. Maeda, Y. Inagaki, H. Suzuki, N. Matsuyama, and H. Fujiwara, "Modeling of the subsurface structure from the seismic bedrock to the ground surface for a broadband strong motion evaluation," J. Disaster Res., Vol.8, No.5, pp. 889-903, 2013.

[28] I. Cho and S. Senna, "Constructing a system to explore shallow velocity structures using a miniature microtremor array – Accumulating and utilizing large microtremor datasets –," Synthesiology!$ Vol.9, No.2!$pp. 86-96, 2016.

[29] T. Satoh, C. J. Poran, K. Yamagata, and J. A. Rodriguez, "Soil profiling by spectral analysis of surface waves," Proc. 2nd Int. Conf. on Recent Advances in Geotechnical Earthquake Engineering and Soil Dynamics, Vol.2, pp. 1429-1434, 1991.

[30] H. Arai and K. Tokimatsu, "S-Wave velocity profiling by inversion of microtremor H/V Spectrum," Bull. Seismol. Soc. Am., Vol.94, pp. 53-63, 2004.

[31] S. Senna, H. Azuma, Y. Murui, and H. Fujiwara, "Development of microtremor survey observation system 'i-bidou' etc.," Proc. of the 124th SEGJ Conf., pp. 346-348, 2011 (in Japanese).

[32] S. Senna, S. Adachi, Y. Asaka, and H. Fujiwara, "Development of a new microtremor survey observation system," Proc. of the 126th SEGJ Conf., pp. 32-34, 2012 (in Japanese).

[33] M. Hori, T. Ichimura, L. Wijerathne, H. Ohtani, J. Chen, K. Fujita and H. Motoyama, "Application of High Performance Computing to Earthquake Hazard and Disaster Estimation in Urban Area," Front. Built Environ., doi: 10.3389/fbuil.2018.00001, 2018.

[34] H. O-tani, M. Hori, and L. Wijerathne, "Automated Model Construction for Seismic Disaster Assessment of Pipeline Network in Wide Urban Area," Earthquakes, Intech, doi: 10.5772/intechopen.78725, 2018.

[35] Iwaizumi Civil Center, Coastal Area Promotion Bureau, Iwate Pref., "Outline of Omoto river improvement plan," p. 6, November, 2016.

[36] [36] T. Ise, T. Isono, Y. Usuda, H. Fujiwara, and K. Yamori, "Study of the Method of Disaster Information Sharing System Considering the Diversity of the Municipalities," Proc. of Institute of Social Safety Science, No.30, pp. 25-34, 2017 (in Japanese).

[37] M. Shiraishi, H. Ashiya, A. Konno, K. Morita, T. Noro, Y. Nomura, and S. Kataoka, "Development of Real-Time Collection, Integration, and Sharing Technology for Infrastructure Damage Information," J. Disaster Res., Vol.14 No.2, 2019.

Name:
Hiroyuki Fujiwara

Affiliation:
Director, Research Center for Reinforcement of Resilient Function, National Research Institute for Earth Science and Disaster Resilience

Address:
3-1 Tennodai, Tsukuba, ibaraki 305-0006, Japan

Brief Career:
1989- Researcher, NIED
2001- Head of Strong Motion Observation Network Laboratory, NIED
2006- Project Director, Disaster Prevention System Research Center, NIED
2011- Director, Social System Research Department, NIED
2014- Director, Research Center for Reinforcement of Resilient Function

Academic Societies & Scientific Organizations:
- Seismological Society of Japan (SSJ)
- Japan Association for Earthquake Engineering (JAEE)

Name:
Hiromitsu Nakamura

Affiliation:
Senior Researcher, Integrated Research on Disaster Risk Reduction Division, National Research Institute for Earth Science and Disaster Prevention (NIED)

Address:
3-1 Tennodai, Tsukuba, Ibaraki 305-0006, Japan

Brief Career:
2001- Researcher, Railway Technical Research Institute
2006- Researcher, NIED
2008- Senior Researcher, NIED
2016- Integrated Research on Disaster Risk Reduction Division, NIED

Selected Publications:
- H. Nakamura et al., "Prototype of a Real-Time System for Earthquake Damage Estimation in Japan," J. Disaster Res., Vol.8, pp. 981-989, 2013.
- A. Kusaka et al., "Bayesian updating of damaged building distribution in post-earthquake assessment," J. of Japan Association for Earthquake Engineering, Vol.17, No.1, pp. 16-29, 2016.

Academic Societies & Scientific Organizations:
- Seismological Society of Japan (SSJ)

Name:
Shigeki Senna

Affiliation:
Principal Research Fellow, Department of Integrated Research on Disaster Prevention, National Research Institute for Science and Disaster Resilience (NIED)

Address:
3-1 Tennodai, Tsukuba, Ibaraki 305-0006, Japan

Brief Career:
1994-2001 Chef Engineer, Dia Consultants Corporation
2001-2003 Chef Engineer, Mitsubishi Space Software Corporation
2003-2014 Researcher, National Research Institute for Earth Science and Disaster Prevention (NIED)
2014- Principal Research Fellow, National Research Institute for Earth Science and Disaster Resilience (NIED)

Selected Publications:
- "Liquefaction during the Kumamoto Earthquakes on April 14and 16, 2016," Lowland Technology Int., Vol.19, No.3, pp. 177-188, 2017.
- "Liquefaction Occurrence Ratio Estimation Considering Strong GroundMotion Duration and Regional Characteristics," J. of Japan Association for Earthquake Engineering, Vol.18, No.2, pp. 82-94, 2018 (in Japanese).

Academic Societies & Scientific Organizations:
- Seismological Society of Japan (SSJ)
- Japan Association for Earthquake Engineering (JAEE)
- Society of Exploration Geophysicists of Japan (SEGJ)

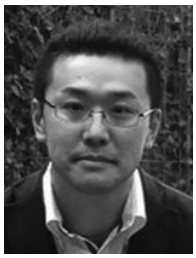

Name:
Hideyuki Otani

Affiliation:
Computational Disaster Mitigation and Reduction Research Team, RIKEN Center for Computational Science

Address:
7-1-26 Minatojima-minami-machi, Chuo-ku, Kobe, Hyogo 650-0047, Japan

Brief Career:
2012 Postdoctral Researcher, RIKEN Advanced Institute for Computational Science
2016- Visiting Associate Professor, University of Hyogo
2017- Research Scientist, RIKEN Center for Computational Science

Selected Publications:
- "Automated Model Construction for Seismic Disaster Assessment of Pipeline Network in Wide Urban Area, Earthquakes," Intech, 2018.

Academic Societies & Scientific Organizations:
- Japan Association for Earthquake Engineering (JAEE)
- Japan Society of Civil Engineers (JSCE)
- GIS Association of Japan (GISA)
- Architectural Institute of Japan (AIJ)

Name:
Naoya Tomii

Affiliation:
Manager for Sarellite Appications, Satellite Appications and Operations Center, Space Technology Directorate I, Japan Aerospace Exploration Agency (JAXA)

Address:
2-1-1 Sengen, Tsukuba, Ibaraki 305-8505, Japan

Brief Career:
1999 Joined National Space Development Agency of Japan (NASDA)
2008- Satellite Appications and Operations Center

Selected Publications:
• "Development of the Monitoring System for Port Facilities using Satellite and SONAR," J. of Ports and Harbours, Vol.92, pp. 30-31, 2015.

Academic Societies & Scientific Organizations:
• Advanced Marine Science and Technology Society (AMSTEC)

Name:
Kiyonori Ohtake

Affiliation:
Executive Researcher, Applications Laboratory, Resilient ICT Research Center, National Institute of Information and Communications Technology

Address:
3-5 Hikaridai, Keihannna Science City, Kyoto 619-0289, Japan

Brief Career:
2001-2006 ATR Spoken Language Translation Research Laboratories
2006 Joined National Institute of Information and Communications Technology

Selected Publications:
• K. Ohtake and E. Mizukami, "NICT Kyoto Dialogue Corpus," N. Ide and J. Pustejovsky (eds.), Handbook of Linguistic Annotation, Springer, pp. 1265-1286, 2017.

Academic Societies & Scientific Organizations:
• Japanese Society for Artificial Intelligence (JSAI)
• Information Processing Society of Japan (IPSJ)
• Association for Natural Language Processing (ANLP)

Name:
Toshiya Mori

Affiliation:
Associate Professor, Geochemical Research Center, Graduate School of Science, The University of Tokyo

Address:
7-3-1 Hongo, Bunkyo-ku, Tokyo 113-0033, Japan

Brief Career:
1994- Research Associate, School of Science, The Uniersity of Tokyo
2004- Associate Professor, Graduate School of Science, The University of Tokyo
1999-2000 Visiting Scientist at Los Alamos National Laboratory

Selected Publications:
• T. Mori and M. Burton, "The SO2 camera: A simple, fast and cheap method for ground-based imaging of SO2 in volcanic plumes," Geophysical Research Letters, Vol.33, L24804, 2006.

Academic Societies & Scientific Organizations:
• Volcanological Society of Japan (VSJ)
• International Association of Volcanology and Chemistry of Earth's Interior (IAVCEI)
• Geochemical Society of Japan (GSJ)

Name:
Shojiro Kataoka

Affiliation:
Head, Earthquake Disaster Management Division, Road Structures Department, National Institute for Land and Infrastructure Management, Ministry of Land, Infrastructure, Transport and Tourism

Address:
1 Asahi, Tsukuba, Ibaraki 305-0804, Japan

Brief Career:
1996- Postdoctoral Researcher, Tokyo Institute of Technology and California Institute of Technology
1998- Research Engineer, Public Works Research Institute
2001- Researcher and Senior Researcher, National Institute for Land and Infrastructure Management
2016- Head, Earthquake Disaster Management Division, National Institute for Land and Infrastructure Management

Selected Publications:
• "Estimation of wave force acting on bridge superstructures due to the 2011 Tohoku Tsunami," J. Disaster Res., Vol.8, No.4, pp. 605-611, 2013.
• "Seismic Design for anti-catastrophe – a study on the implementation as design codes –," J. of JSCE, Vol.5, pp. 346-356, 2017.

Academic Societies & Scientific Organizations:
• Japan Society of Civil Engineers (JSCE)
• Japan Association for Earthquake Engineers (JAEE)